Inhibition of $K_{Ca}2.2$ and $K_{Ca}2.3$ channel currents by protonation of outer pore histidine residues

Samuel J. Goodchild,[1] Cedric Lamy,[2] Vincent Seutin,[2] and Neil V. Marrion[1]

[1]Department of Physiology and Pharmacology, School of Medical Sciences, University of Bristol, Bristol BS8 1TD, England, UK

[2]Laboratory of Pharmacology, Giga-Neurosciences, University of Liège, 4000 Liège, Belgium

Ion channels are often modulated by changes in extracellular pH, with most examples resulting from shifts in the ionization state of histidine residue(s) in the channel pore. The application of acidic extracellular solution inhibited expressed $K_{Ca}2.2$ (SK2) and $K_{Ca}2.3$ (SK3) channel currents, with $K_{Ca}2.3$ (pIC_{50} of ~6.8) being approximately fourfold more sensitive than $K_{Ca}2.2$ (pIC_{50} of ~6.2). Inhibition was found to be voltage dependent, resulting from a shift in the affinity for the rectifying intracellular divalent cation(s) at the inner mouth of the selectivity filter. The inhibition by extracellular protons resulted from a reduction in the single-channel conductance, without significant changes in open-state kinetics or open probability. $K_{Ca}2.2$ and $K_{Ca}2.3$ subunits both possess a histidine residue in their outer pore region between the transmembrane S5 segment and the pore helix, with $K_{Ca}2.3$ also exhibiting an additional histidine residue between the selectivity filter and S6. Mutagenesis revealed that the outer pore histidine common to both channels was critical for inhibition. The greater sensitivity of $K_{Ca}2.3$ currents to protons arose from the additional histidine residue in the pore, which was more proximal to the conduction pathway and in the electrostatic vicinity of the ion conduction pathway. The decrease of channel conductance by extracellular protons was mimicked by mutation of the outer pore histidine in $K_{Ca}2.2$ to an asparagine residue. These data suggest that local interactions involving the outer turret histidine residues are crucial to enable high conductance openings, with protonation inhibiting current by changing pore shape.

The Journal of General Physiology

INTRODUCTION

The $K_{Ca}2.2$ (SK2) and $K_{Ca}2.3$ (SK3) potassium channels are characterized by their activation by intracellular calcium (Ca^{2+}; half-maximal activation of 0.3–0.7 µM), voltage independence, and small single-channel conductance of 10–20 pS (Köhler et al., 1996; Hirschberg et al., 1998; Xia et al., 1998). Because of the distinct spatial distribution of the channel subtypes in the mammalian brain and their involvement in the generation of afterhyperpolarization currents, there has been considerable interest in developing subtype-selective pharmacological tools to study these channels (Stocker and Pedarzani, 2000; Shakkottai et al., 2001; Sailer et al., 2002, 2004; Stocker et al., 2004; Dilly et al., 2005). The predicted pore regions of $K_{Ca}2.2$ and $K_{Ca}2.3$ display high sequence homology. Each channel subunit possesses a histidine (H) residue that is predicted to reside within the extracellular-facing region of the outer pore (H337 in $K_{Ca}2.2$ and H491 in $K_{Ca}2.3$). In addition, the $K_{Ca}2.3$ subunit exhibits an additional H (H522) that is seen as asparagine (N368) in $K_{Ca}2.2$. Histidine residues in channels' outer pore regions have been reported to be proton interaction sites that mediate inhibition of currents. For example, proton-induced inhibition is observed for several different potassium channels, including the voltage-gated *Shaker*-like plant channel ATK3 (Geiger et al., 2002), Kv1.5 (Steidl and Yool, 1999; Jäger and Grissmer, 2001; Kehl et al., 2002), Kv1.4 (Claydon et al., 2000), Kv7.2/7.3 (Prole et al., 2003), $K_{2P}2.1$ (Cohen et al., 2008), and the inward-rectifying channel Kir2.3 (Coulter et al., 1995; Ureche et al., 2008). Several mechanisms have been proposed to explain this inhibition. For example, Kv1.5 macroscopic current block is mediated through modifying gating and enhancing inactivation without any effect on single-channel conductance (Kwan et al., 2006). Macroscopic inhibition of both ATK3 and Kir2.3 channel currents resulted from a reduction in single-channel conductance (Coulter et al., 1995; Geiger et al., 2002), whereas inhibition of Kv7.2/7.3 heteromeric channel currents resulted from both effects on gating and single-channel conductance (Prole et al., 2003).

We demonstrate that macroscopic $K_{Ca}2.2$ and $K_{Ca}2.3$ current is inhibited by extracellular protons, with $K_{Ca}2.3$ being more sensitive. Inhibition resulted from a reduction in single-channel conductance and, in particular for $K_{Ca}2.3$, a shift of inward rectification. We show that

V. Seutin and N.V. Marrion contributed equally to this paper.

Correspondence to Neil V. Marrion: N.V.Marrion@bris.ac.uk

Abbreviation used in this paper: GHK, Goldman-Hodgkin-Katz.

The Rockefeller University Press $30.00
J. Gen. Physiol. Vol. 134 No. 4 295–308
www.jgp.org/cgi/doi/10.1085/jgp.200910252

the outer pore histidine residues in the $K_{Ca}2.2$ and $K_{Ca}2.3$ channel act as proton sensors. The observed significant differences in modulation between the two subtypes provide insight into the role of such outer pore residues in channel function that might aid the development of subtype-selective modulators.

MATERIALS AND METHODS

Cell culture, expression of channels, and mutagenesis

Wild-type rat $K_{Ca}2.2$ (GenBank accession no. NM_019314) and human $K_{Ca}2.3$ (GenBank accession no. AF031815) channel DNA were subcloned into the mammalian plasmid expression vectors pcDNA3 (Invitrogen) and pFlagCMV2 (Sigma-Aldrich), respectively. Point mutations in $K_{Ca}2.2$ ($K_{Ca}2.2$(N368H), $K_{Ca}2.2$(H337N), and $K_{Ca}2.2$(H337N, N368H)) and $K_{Ca}2.3$ ($K_{Ca}2.3$(H522N) and $K_{Ca}2.3$(H421N)) were introduced using a site-directed mutagenesis kit (Quickchange-XL; Agilent Technologies) and confirmed by dye termination DNA sequencing.

Channels were transiently expressed in HEK293 cells for electrophysiology. Cells were dissociated for passage using an EDTA solution and maintained in Dulbecco's modified Eagle's medium, supplemented with 10% fetal calf serum and 1% penicillin/streptomycin (all from Invitrogen) at 37°C. Cells were plated onto 35-mm dishes (BD) 48 h before transfection for electrophysiology. Transient transfections of HEK293 cells were made using polyethylenimine (Johnson Matthey Plc) by combining channel plasmid DNA with enhanced green fluorescent protein DNA in a ratio of 1:1 to 1:10 (maximum plasmid content, 1 µg). Cells expressing enhanced green fluorescent protein were used for electrophysiology 12–24 h after transfection.

Electrophysiology

Solutions. Expressed macroscopic currents were resolved using either whole cell or outside-out macropatch recording, with cells/patches being constantly superfused with external solutions of 160 or 5 mM potassium ($[K^+]_o$). The composition of the 160 mM K^+ (high K^+) solution was (in mM): 120 KCl, 10 HEPES, 10 EGTA, 1.44 $MgCl_2$, and 6.19 $CaCl_2$ (achieving a buffered concentration of 60 nM Ca^{2+} and 1 mM Mg^{2+}), with the pH adjusted to 7.4 with ~40 mM KOH. Extracellular Ca^{2+} and Mg^{2+} were set at this level to minimize concentration gradients for the divalent ions. Acidic solutions (pH <7.4) contained (in mM): 120 KCl, 10 KMes, 10 EGTA, 1.44 $MgCl_2$, and 6.19 $CaCl_2$, pH adjusted with KOH. The composition of the 5-mM K^+ (low K^+) solution was (in mM): 110 NaCl, 5 KCl, 10 HEPES(Na), 10 EGTA, 1.44 $MgCl_2$, and 6.19 $CaCl_2$ (achieving a buffered concentration of 60 nM Ca^{2+} and 1 mM Mg^{2+}), with the pH adjusted to 7.4 with ~23 mM NaOH. Acidic low K^+ solutions contained (in mM): 110 NaCl, 5 KMes, 10 EGTA, 1.44 $MgCl_2$, and 6.19 $CaCl_2$, pH adjusted with NaOH.

Whole cell and macropatch recording electrodes were fabricated from KG-33 glass (Friedrich & Dimmock, Inc.) and filled with a solution of composition (in mM): 120 KCl, 10 HEPES, 10 BAPTA, 1.5 ATP(Na_2), 2.34 $MgCl_2$, and 8.98 $CaCl_2$ (added to achieve 1 µM free Ca^{2+}), pH 7.4, which gave resistances of 2–4 MΩ. Zn^{2+} solutions were prepared from a 500-mM stock (pH of ~2), and the pH was adjusted to 7.4 with KOH. Zn^{2+} in solution can form the insoluble $ZnOH_2$, therefore limiting the maximum solubility of Zn^{2+} at pH 7.4 to 4.5 mM.

Electrodes contained a high K^+ solution for excised inside-out single-channel Ca^{2+} activation and noise analysis recordings of the following composition (in mM): 97 K aspartate or K methylsulfate ($MeSO_4$), 30 KCl, 10 HEPES, 10 EGTA, 1.44 $MgCl_2$, and 6.19 $CaCl_2$ (achieving a buffered concentration of 60 nM Ca^{2+} and 1 mM Mg^{2+}), with the pH adjusted to 7.4 with KOH. The intracellular side of excised inside-out patches was bathed in the same high K^+ solution, with free Ca^{2+} buffered to 60 nM, 200 nM (adding 1.18 $MgCl_2$ and 8.445 $CaCl_2$), 300 nM (adding 1.12 $MgCl_2$ and 8.9 $CaCl_2$), 600 nM (adding 1.07 $MgCl_2$ and 9.4 $CaCl_2$), or 1 µM (adding 1.04 $MgCl_2$ and 9.64 $CaCl_2$). The effect of extracellular acidic pH on single-channel and noise analysis recordings was studied with the electrode containing the high K^+ solution, which was buffered to the stated pH by replacing HEPES with Mes.

The liquid junction potential calculated between high K^+ solutions was <2 mV, whereas that between low K^+ external solutions and electrode solution was calculated to be ~8 mV. Neither was corrected for. All standard chemicals were bought from Sigma-Aldrich.

Recording

Whole cell and macropatch currents were recorded with an Axopatch 200A (MDS Analytical Technologies). Capacitance and series resistance compensation (≥95%) was only used for whole cell recordings. Currents were low-pass filtered at 1 kHz (eight-pole Bessel; Frequency Devices, Inc.) and acquired at 20 kHz using Pulse (HEKA). All recordings were performed at room temperature (20–25°C). Extracellular solutions were exchanged by a whole bath perfusion system for pH experiments, with a rapid solution exchange system (RSC200; Biologic) used for noise analysis. A long-lasting current run-up was sometimes observed after current was inhibited by acidic extracellular pH (not depicted). Current amplitude was stabilized after returning to pH 7.4 and only accepted for analysis if the inhibition was reversible. Electrodes for single-channel recording were fabricated from quartz capillary (King Precision Glass, Inc.), with resistances of 7–12 MΩ. Single-channel currents were observed by continuous recording at all potentials. Channel currents were filtered at 1 kHz and acquired at 20 kHz using the Pulse program. Single-channel activity was analyzed with TAC (Bruxton) using the 50% threshold technique, and all transitions were visually inspected before being accepted. Single-channel amplitudes were estimated from Gaussian fits of amplitude histograms derived from events >1 ms to account for the rise time of the Bessel filter.

Data analysis

Concentration–inhibition relationships to extracellular protons (H^+) were plotted as fractional current remaining (I/I_{cont}) and were fitted with a Hill equation of the form:

$$\frac{I}{I_{cont}} = A_1 + \frac{A_2 - A_1}{1 + 10^{((Log(IC50) - [H^+])n_h))}}, \quad (1)$$

where I was the recorded macroscopic current, I_{cont} the current at pH 7.4, A_1 the minimum fraction of current remaining, A_2 the maximum, and IC_{50} the concentration in molar of protons that evoked 50% of the maximum inhibition. The IC_{50} concentration is also quoted as $-\log IC_{50}$ (pIC_{50}) in the text. Unless stated otherwise, fitting was performed on data from individual experiments, and the fit parameters quoted are of the mean ± SEM of the individual fits. For display purposes, figures show Eq. 1 fitted to mean data. Fitting was performed using Prism (GraphPad Software, Inc.).

Nonstationary noise analysis

Excised inside-out macropatches were held at −50 mV. Currents were acquired using Pulse (HEKA), and only sweeps without artifacts from the solution exchange system were accepted. Mean current (I) and variance (σ^2) were calculated for each ensemble of current traces using Clampfit (MDS Analytical Technologies). The single-channel current (i) and the number of channels (N)

in each patch were then obtained by fitting a plot of the variance against the mean current using Eq. 2 (Sigworth, 1980; Hartveit and Veruki, 2007):

$$\sigma^2 = iI - \frac{I^2}{N}. \quad (2)$$

Single-channel conductance (γ) and maximum open probability at the maximum mean I (P(o)) were calculated. Curve fitting of equations to the data were performed using Origin software (OriginLab Corp.). Statistical significance was evaluated using Prism (GraphPad Software, Inc.) by either the Student's *t* test or one- or two-way ANOVA with Bonferroni post hoc test as appropriate.

The validity of applying this analysis to $K_{Ca}2$ channel activity was tested by simulation of three different gating schemes using CSIM (MDS Analytical Technologies; see Fig. 4 for gating schemes). Simulated deactivation current relaxations (128) were generated for each gating scheme using 80 independent channels, except for the scheme in Fig. 4 B, which used 40 channels of high conductance and 40 channels of low conductance. Each simulation used the open channel as the initial state. Transition rates shown in Fig. 4 were obtained from Hirschberg et al. (1998). Data were analyzed in the same manner as experimentally derived data using Clampfit. Amplitude histograms were produced by running the simulation of each gating scheme with one channel, with data analyzed in the same way as experimentally derived data using TAC and TACFit.

Homology model construction

Putative locations of pore residues were predicted based on a model of the $K_{Ca}2.2$ pore region. The pore region of $K_{Ca}2.2$ spanning S5-Phelix-SF-S6 was modeled using the mammalian Kv1.2 pore (PDB: 2a79) (Long et al., 2005) as a template through the comparative modeling web server, Geno 3D (Combet et al., 2002).

RESULTS

Extracellular protons ($[H^+]_o$) inhibited $K_{Ca}2.2$ and $K_{Ca}2.3$ macroscopic currents

Ramp currents from outside-out macropatches with an intracellular Ca^{2+} concentration of 1 µM showed inwardly rectifying $K_{Ca}2.2$ and $K_{Ca}2.3$ currents, which were inhibited differentially by increasing concentrations of extracellular protons ($[H^+]_o$) (Fig. 1 A). $K_{Ca}2.3$ currents showed a greater sensitivity to $[H^+]_o$ than the $K_{Ca}2.2$-mediated current, with the $K_{Ca}2.3$ current being inhibited by pH 6.6 while the $K_{Ca}2.2$ current was unaffected. The effect of $[H^+]_o$ appeared to be voltage dependent, with inhibition being most apparent at potentials negative to 0 mV (Fig. 1 B). Inhibition at −60 mV by decreasing extracellular pH was plotted for both $K_{Ca}2.2$ and $K_{Ca}2.3$. The maximum inhibition by pH 5.5 was significantly greater for $K_{Ca}2.3$ currents (78 ± 0.1%; $n = 4$) than that observed for $K_{Ca}2.2$ currents (44 ± 2.0%; $n = 3$; $P < 0.0005$). Fitting the data with the Hill equation showed the higher sensitivity of $K_{Ca}2.3$ to $[H^+]_o$ (IC_{50} = 158 nM and pIC_{50} = 6.8 nM; $n_h = -2.1 \pm 0.1$ and $n = 4$–11) compared with inhibition of the $K_{Ca}2.2$ current (IC_{50} = 63 nM and pIC_{50} = 6.2 nM; $n_h = -1.9 \pm 0.1$ and $n = 3$; pIC_{50}, $P < 0.0001$; n_h, not significant). The steep Hill slopes for $K_{Ca}2.2$ and $K_{Ca}2.3$ suggest that more than one proton binds to inhibit current and positive cooperativity exists for inhibition.

Although potential effects of extracellular pH on the determined levels of intracellular Ca^{2+} were controlled

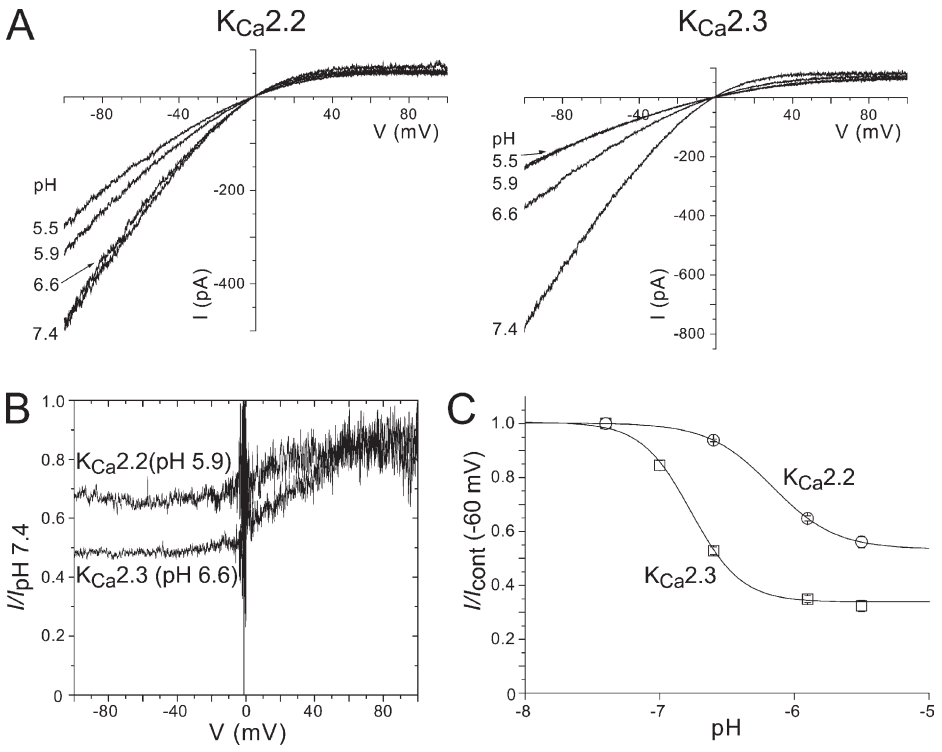

Figure 1. Differential inhibition of $K_{Ca}2.3$ and $K_{Ca}2.2$ channel macroscopic current by increasing $[H^+]_o$. (A) Representative outside-out macropatch $K_{Ca}2.2$ and $K_{Ca}2.3$ currents evoked by voltage ramps from −100 to +100 mV over 1 s in control conditions (pH 7.4) and in pH 6.6, 5.9, and 5.5. (B) Inhibition was voltage dependent, with less inhibition observed at depolarized levels. This was apparent when the fraction of unblocked current ($K_{Ca}2.2$, $I_{pH5.9}/I_{pH7.4}$; $K_{Ca}2.3$, $I_{pH6.6}/I_{pH7.4}$) was plotted against membrane voltage for $K_{Ca}2.2$ and $K_{Ca}2.3$ currents shown in A, indicating that block negative to 0 mV was voltage independent, and less inhibition was observed as the membrane potential approached +100 mV. (C) Concentration–inhibition relationships for the inhibition of $K_{Ca}2.2$ and $K_{Ca}2.3$ by $[H^+]_o$. Data points from different patches (n = 3–11) were fit with Eq. 1.

for by using intracellular BAPTA, it was possible that the reduction of macroscopic $K_{Ca}2$ current resulted from a change in the Ca^{2+}-dependent gating of channels. Inside-out macropatches with electrodes containing either pH 7.4 or 5.9 were exposed to increasing intracellular concentrations of free Ca^{2+} to determine the effects on Ca^{2+}-dependent gating. Extracellular acidosis had no significant effect (unpaired *t* test; $n = 3–5$ patches)

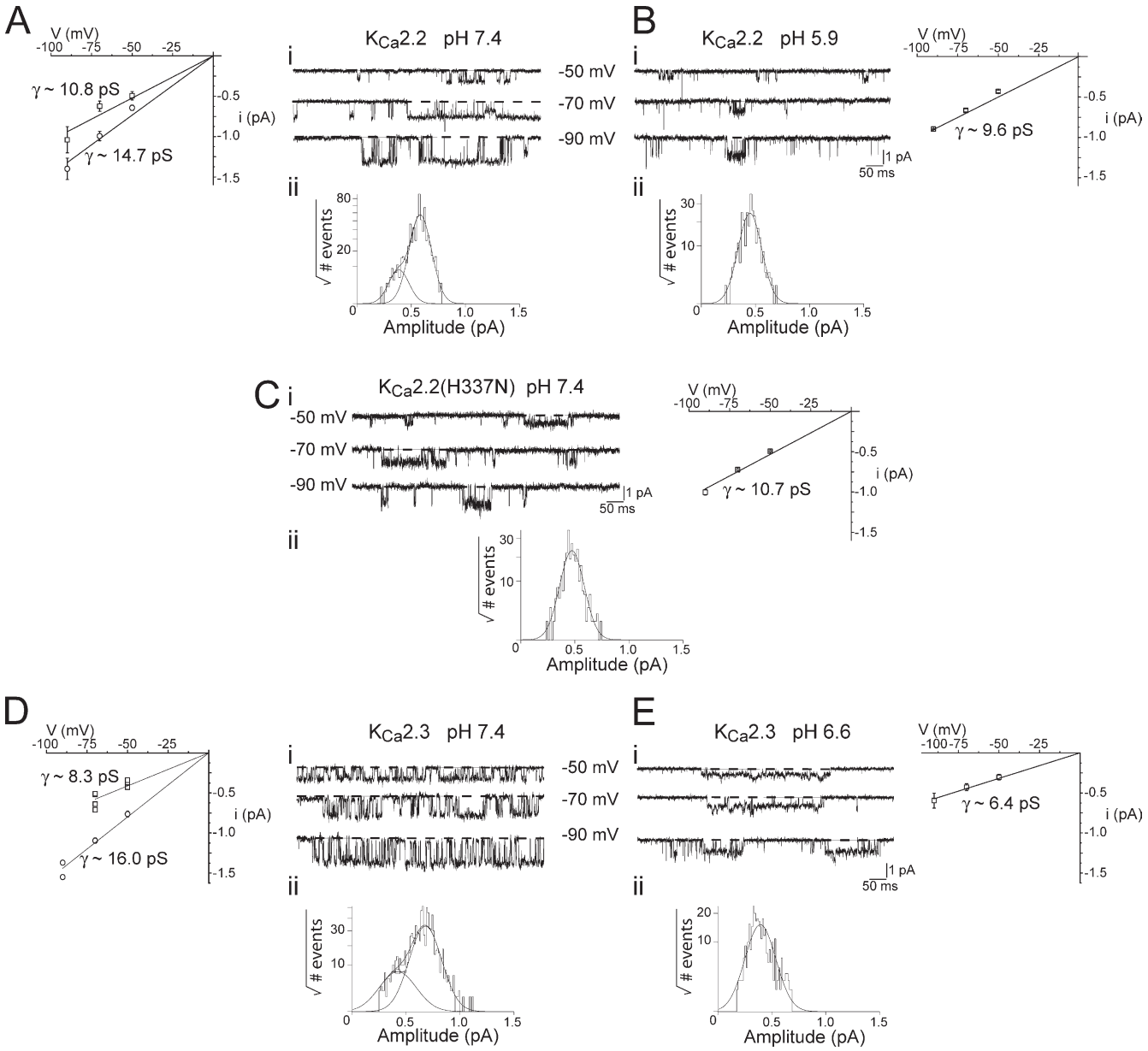

Figure 2. Extracellular acidosis reduced single $K_{Ca}2.2$ and $K_{Ca}2.3$ channel conductance. (A, i) Single $K_{Ca}2.2$ channel activity at extracellular pH 7.4 in the presence of 200 nM of intracellular Ca^{2+} at −50, −70, and −90 mV. (Left) Current–voltage relationship showing that $K_{Ca}2.2$ channels exhibited two conductance levels of ∼15 and 11 pS. (A, ii) Amplitude histogram of channel openings at −50 mV, with mean amplitudes of 0.58 and 0.39 pA. (B, i) Acidification of the pipette (external) solution to pH 5.9 resulted in lower conductance openings. (Right) $K_{Ca}2.2$ channels exhibited only one conductance level in pH 5.9 of ∼9.63 pS. (B, ii) Amplitude histogram of channel openings at −50 mV, with a mean amplitude of 0.45 pA. (C, i) Single $K_{Ca}2.2$(H337N) channel openings at extracellular pH 7.4 of low amplitude. (Right) Current–voltage relationship showing that the mutant channel exhibited only low conductance openings of 10.7 pS. (C, ii) Amplitude histogram of channel openings at −50 mV, with a mean amplitude of 0.47 pA. (D, i) Single $K_{Ca}2.3$ channel openings at extracellular pH 7.4 activated by 200 nM of intracellular Ca^{2+} at −50, −70, and −90 mV. (Left) $K_{Ca}2.3$ channels exhibited two conductance levels of ∼16 and 8 pS. (D, ii) Amplitude histogram of channel openings at −50 mV, with mean amplitudes of 0.68 and 0.41 pA. (E, i) $K_{Ca}2.3$ channels only exhibited low conductance openings in pH 6.6. (Right) Current–voltage relationship showing that conductance was ∼6.5 pS in extracellular pH 6.6. (E, ii) Amplitude histogram of channel openings at −50 mV, with a mean amplitude of 0.37 pA.

on EC_{50} or Hill slopes for either $K_{Ca}2.2$ (pH 7.4, EC_{50} = 281 ± 29 nM and n_h = 5.98 ± 1.27; pH 5.9, EC_{50} = 231 ± 15 nM and n_h = 6.21 ± 0.96) or $K_{Ca}2.3$ (pH 7.4, EC_{50} = 257 ± 21 nM and n_h = 5.22 ± 0.55; pH 5.9, EC_{50} = 284 ± 12 nM and n_h = 5.86 ± 0.24) current, indicating that inhibition by protons was independent of changes in the mechanics of Ca^{2+} gating. These data suggested that inhibition of macroscopic current might have resulted from changes in single-channel properties.

Extracellular protons inhibited $K_{Ca}2$ current by decreasing single-channel conductance

Extracellular protons were proposed to inhibit Kv1.5 current by reducing channel P(o) (Kwan et al., 2006). In contrast, a reduction in single-channel conductance was suggested to underlie the inhibition of inward-rectifying K^+ current (Coulter et al., 1995; Geiger et al., 2002). We used a combination of single-channel recording and nonstationary noise analysis to resolve which channel property might be affected to underlie the inhibition of macroscopic $K_{Ca}2$ current. Excised inside-out recording of $K_{Ca}2.2$ and $K_{Ca}2.3$ channels showed in extracellular pH 7.4 that both channels exhibited two conductance levels of 15 and 11 pS for $K_{Ca}2.2$ channels (14.7 ± 1.1 and 10.8 ± 1.4 pS; n = 3) (Fig. 2 A) and 16 and 8 pS for $K_{Ca}2.3$ (15.8 ± 0.6 and 8.3 ± 0.6 pS; n = 5 and 3) (Fig. 2 D), respectively. Both amplitudes were observed in patches that contained single-level activity bathed in 200 nM Ca^{2+}, and rare transitions between open states were resolved (Fig. 2 A). Recording single-channel activity at the extracellular pH that was close to the determined IC_{50} values showed that conductance was reduced for both channel subtypes by extracellular acidosis, with only a 10-pS (9.6 ± 0.07 pS; n = 3) and a 6.5-pS (6.4 ± 0.8 pS; n = 4) conductance level observed for $K_{Ca}2.2$ channels and $K_{Ca}2.3$ channels, respectively

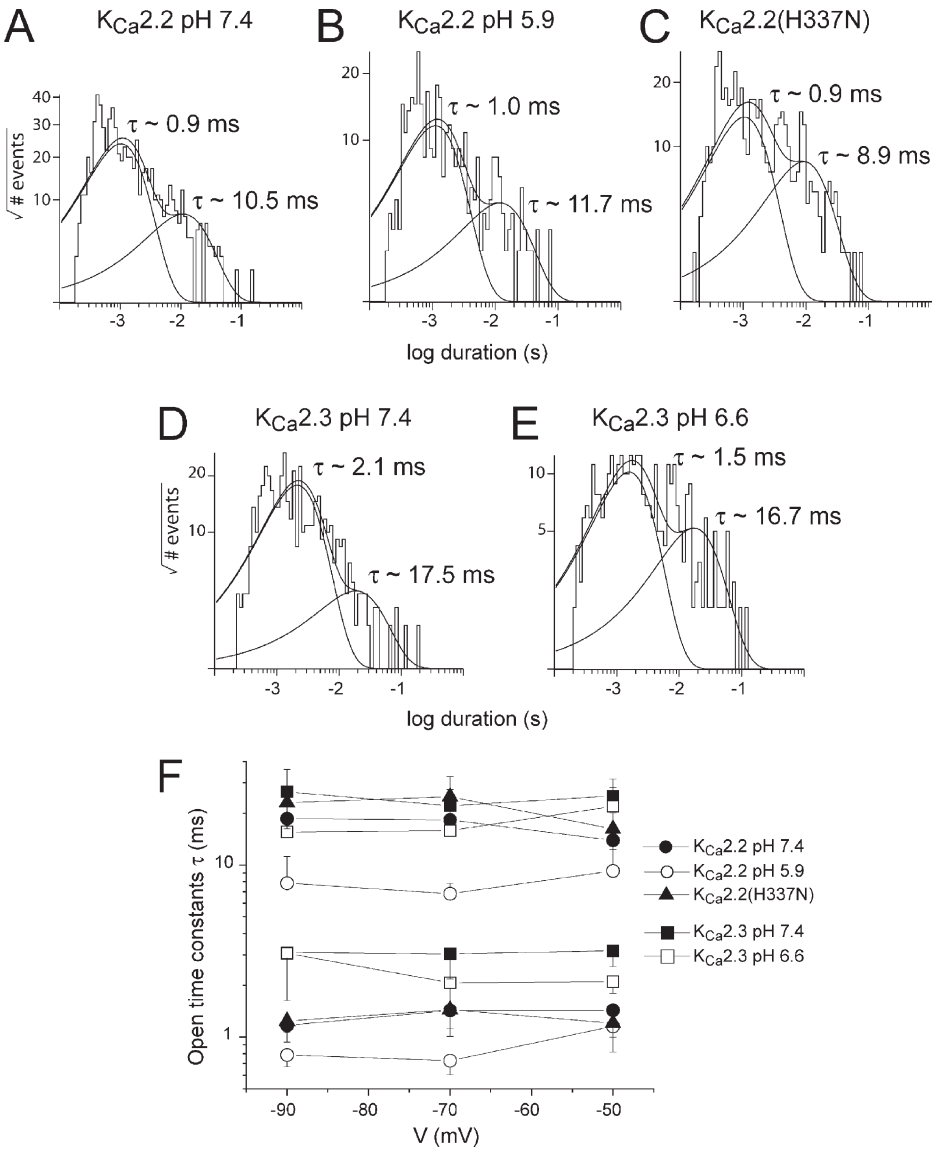

Figure 3. $K_{Ca}2.2$ and $K_{Ca}2.3$ channel open-state kinetics were not changed by extracellular acidosis. Open-time histograms for all single-level openings of both amplitudes at −50 mV from patches containing (A) $K_{Ca}2.2$ in extracellular pH 7.4, (B) $K_{Ca}2.2$ in pH 5.9, (C) $K_{Ca}2.2$(H337N) in pH 7.4, (D) $K_{Ca}2.3$ in pH 7.4, and (E) $K_{Ca}2.3$ in pH 6.6. Distributions were best fit by the sum of two exponentials with τ of 1 and 11 ms for $K_{Ca}2.2$ and 2 and 17 ms for $K_{Ca}2.3$. (F) Mean open times for $K_{Ca}2.2$ and $K_{Ca}2.3$ channel openings at pH 7.4 and 5.9, and those of the mutant $K_{Ca}2.2$ (H337N) channel were plotted against voltage (n = 3). Each open-time component was voltage independent (one-way ANOVA; $P > 0.05$) and were not affected by lowering the extracellular pH (two-way repeated measures ANOVA; $P > 0.05$).

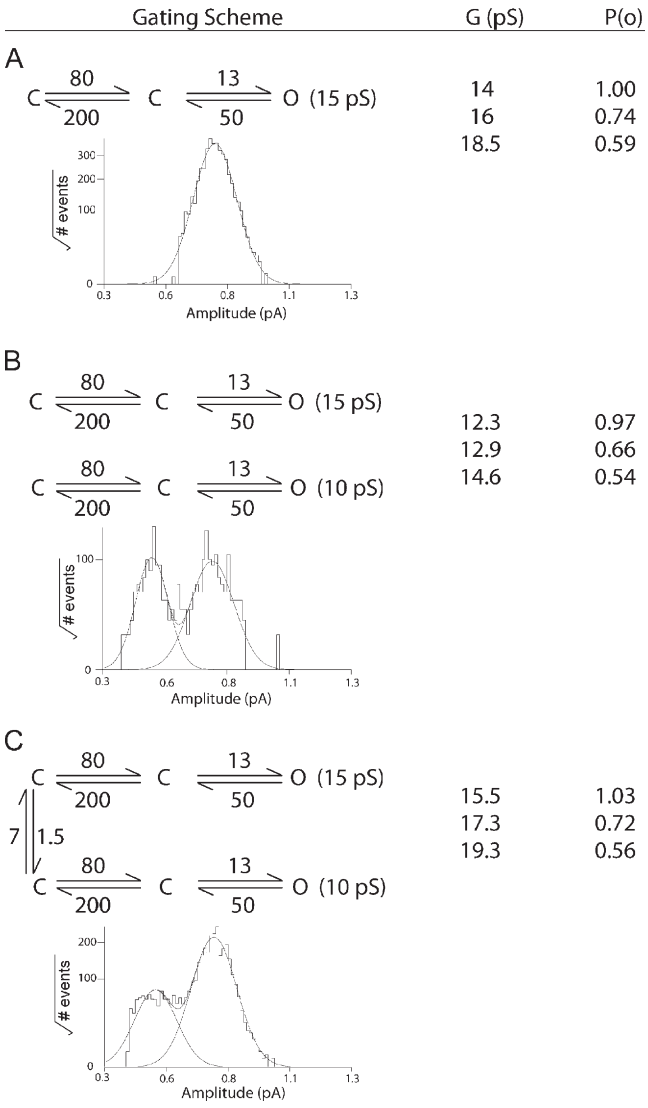

Figure 4. Validity of applying nonstationary noise analysis to $K_{Ca}2$ channel currents. Simulated deactivation currents using the three illustrated gating schemes were subjected to mean-variance analysis to obtain estimates of channel conductance and P(o). Estimates were obtained for three time points in the deactivation 0.3, 10, and 20 ms after the start of the relaxation. These data showed that nonstationary noise analysis can be applied to data obtained from a channel that exhibited two conductance states, such as $K_{Ca}2.2$ and $K_{Ca}2.3$ channels (see Fig. 2).

(Fig. 2, B and E). The observed conductances were not significantly different from the lower conductance class observed in pH 7.4, suggesting that extracellular protons promoted the lower conductance state at the expense of the higher conductance state. These data suggested that the promotion of low amplitude openings was a significant contributor to the reduction of macroscopic current.

Excised inside-out patches usually contained multiple channels that were revealed by observing channel activity in the presence of 1 μM Ca^{2+}, which is close to the maximum for $K_{Ca}2$ activation and correlated with a P(o) of ~0.6–0.8 (Hirschberg et al., 1998; Xia et al., 1998). Lower activity (giving single-level openings) was obtained by bathing patches in 200 nM free Ca^{2+}, and the effect of extracellular pH on open-state kinetics was determined under these conditions to resolve whether the reduction of macroscopic current might be contributed by a decrease in channel open time. $K_{Ca}2.2$ and $K_{Ca}2.3$ channel open-state kinetics were best described by the sum of two exponentials, with τ of ~1–2 and 11–17 ms at extracellular pH 7.4 (Fig. 3, A and D). Analysis of openings in pH 5.9 and 6.6 gave open-state histograms that were best fit with the sum of two exponentials of similar τ (Fig. 3, B and E). Plotting the mean values for each open-time component against membrane voltage showed that channel open-state kinetics were independent of voltage (Hirschberg et al., 1998), and that extracellular protons had no significant effect on open-state kinetics (one-way ANOVA; $P > 0.05$) (Fig. 3 F).

Channel P(o) was extremely difficult to reliably obtain with multichannel patches containing low amplitude openings promoted by lowering extracellular pH. We wanted to use nonstationary noise analysis to get estimates of P(o), together with weighted single-channel amplitude (i) and total number of channels active in a patch (N). It was important to determine whether this technique could be applied to a channel that displayed two amplitude levels by using simulated channel data derived from three gating schemes (Fig. 4). Estimates of channel conductance and P(o) were taken from three time points during the deactivation of a simple C-C-O scheme of conductance of 15 pS (Fig. 4 A). Channel conductance was reasonably well estimated with this technique, with most error occurring when P(o) was lowest. In contrast, channel conductance was not well estimated when noise was contributed by two classes of channels, with conductances of 10 and 15 pS (Fig. 4 B). Importantly, differences in estimated P(o) were noted between this scheme and the scheme in Fig. 4 A. Finally, the scheme in Fig. 4 C was used where a channel exhibited two amplitude levels to replicate that observed for both $K_{Ca}2.2$ and $K_{Ca}2.3$ channels. This gating scheme gave estimated P(o) values that were very similar to those seen with the scheme in Fig. 4 A. Analysis of these simulated data showed that nonstationary noise analysis could be applied to $K_{Ca}2$ channel activity to obtain estimates of P(o).

Expressed $K_{Ca}2.2$ or $K_{Ca}2.3$ channels were repeatedly activated by rapid application of 1 μM Ca^{2+} to excised inside-out macropatches. The variance was calculated from the deactivation relaxation evoked by the rapid removal of 1 μM Ca^{2+} (Fig. 5, A–C). Plotting the variance (σ) against mean current (I) produced a relationship fit with Eq. 2, yielding estimates of single-channel conductance (γ) (Fig. 5 C), P(o) (Fig. 5 D), and N. Decreasing

the extracellular pH from 7.4 to 5.5 reduced γ of $K_{Ca}2.2$ channels from 23.6 ± 5.7 to 10.3 ± 0.6 pS ($P < 0.05$; $n = 3$) (Fig. 5 C). Similar decreases in γ by pH 5.5 were observed for $K_{Ca}2.3$ channels, where it decreased from 24.1 ± 4.9 pS at pH 7.4 to 6.04 ± 1.4 pS in pH 5.5 ($P < 0.03$; $n = 3$) (Fig. 5 C). These data are consistent with the estimates of single $K_{Ca}2.2$ and $K_{Ca}2.3$ channel conductances in the presence of both pH 7.4 and 5.5 (Fig. 2). Channel P(o) activated by 1 µM Ca^{2+} for both subtypes was estimated to be 0.7 ± 0.1 ($n = 3$) for $K_{Ca}2.2$ at pH 7.4 and 0.8 ± 0.09 at pH 5.5, and 0.81 ± 0.05 for $K_{Ca}2.3$ at pH 7.4 and 0.73 ± 0.04 at pH 5.5 (no significant difference) (Fig. 5 D), showing that extracellular protons did not affect channel P(o). These data show that neither changes in open-state kinetics nor channel P(o) underlie the inhibition of macroscopic current by extracellular protons, suggesting that the promotion of low conductance openings was the principal mechanism underlying inhibition.

A histidine residue in the S5-P helix outer pore region was required for current inhibition

The amino acid sequences of $K_{Ca}2.2$ and $K_{Ca}2.3$ channels were aligned, and the predicted extracellular pore regions of the channel were examined for residues that could be ionized by increasing extracellular $[H^+]_o$. Histidine (H) residues are weakly basic (pK_a of ~6), acquiring a single-positive charge by protonation across the pH range that has been examined (pH 7.4–5.5). Fig. 6 displays the pore region sequence alignment of the channels with the H residues highlighted. Both channels share an H residue in homologous positions in the outer pore region (H337 in $K_{Ca}2.2$ and H491 in $K_{Ca}2.3$) (Fig. 6, A–C), and it was hypothesized that the protonation of H337 of $K_{Ca}2.2$ and H491 in $K_{Ca}2.3$ underlay the inhibition of macroscopic current by extracellular protons. Mutation of H to the polar but unionizable asparagine residue (N) was done in both $K_{Ca}2.2$(H337N) and $K_{Ca}2.3$(H491N). The application of extracellular

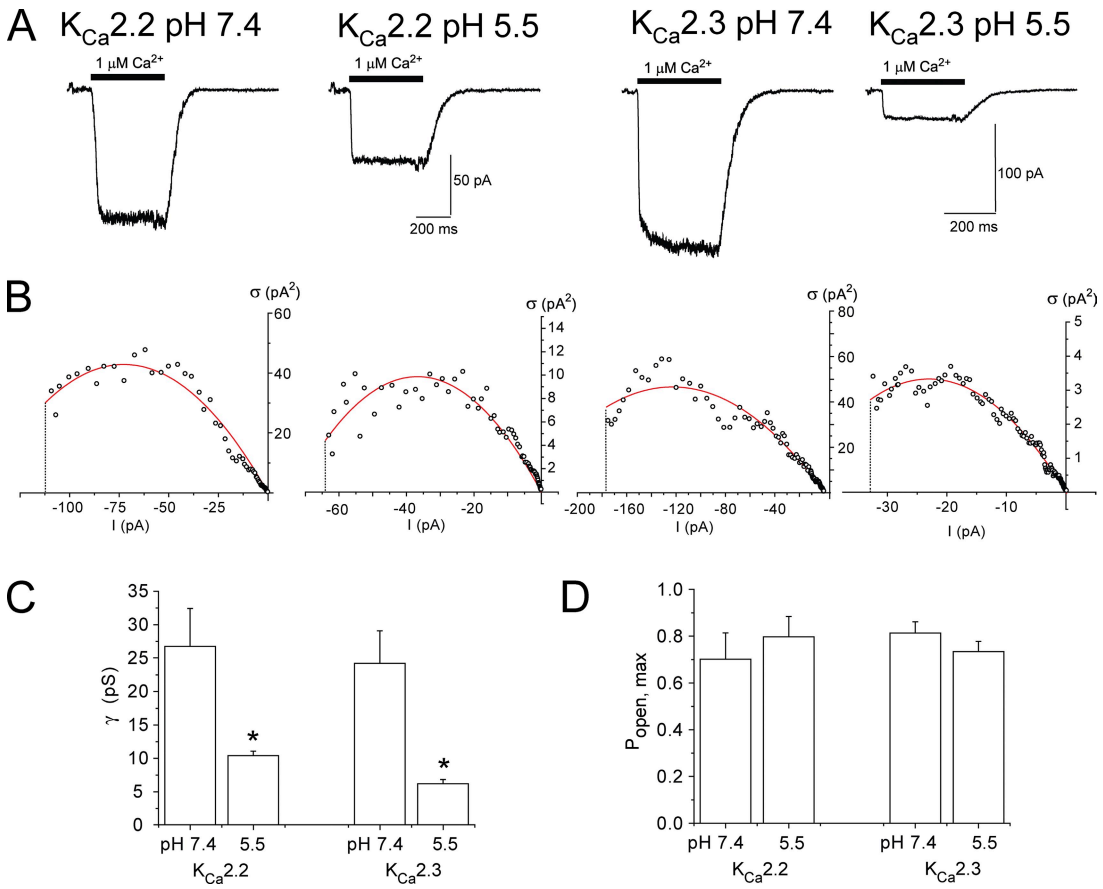

Figure 5. $K_{Ca}2.2$ and $K_{Ca}2.3$ channel P(o) was not affected by extracellular $[H^+]_o$. Nonstationary noise analysis of $K_{Ca}2.2$ and $K_{Ca}2.3$ channel currents in extracellular pH 7.4 or 5.5 was used to estimate channel P(o). (A) Representative traces from inside-out macropatches containing $K_{Ca}2.2$ or $K_{Ca}2.3$ channels in different external pHs held at −50 mV. Patches were bathed in 60 nM Ca^{2+}, and current was activated by rapid application of 1 µM Ca^{2+} for 500 ms. (B) Plots of variance (σ^2) against mean current (I) were fit with Eq. 2 to give estimates of single-channel amplitude (i), which were converted to conductance (γ) using $\gamma = i/V$. Channel P(o) was calculated from I_{max}/Ni. Plots are data reduced for clarity, and curve-fitting procedures were performed on full datasets. (C) Nonstationary noise analysis estimates for γ showed a significant reduction evoked by pH 5.5 for $K_{Ca}2.2$ ($n = 3$; $P < 0.05$) and $K_{Ca}2.3$ ($n = 3$; $P < 0.03$). (D) Neither $K_{Ca}2.2$ nor $K_{Ca}2.3$ channel P(o) was changed by extracellular pH 5.5.

pH 5.5 to either mutant had very little effect on macroscopic current (Fig. 6, D and E). Full concentration–inhibition relationships for both mutants showed that they exhibited significantly reduced sensitivity to $[H^+]_o$ over the pH range of 7.4 to 5.5 (Fig. 6 F). These data indicated that the outer pore H common to both channel subtypes was the molecular target for titration by protons.

Previous data showed that extracellular protons did not inhibit $K_{Ca}2.2$ or $K_{Ca}2.3$ currents by reducing the sensitivity of the channel to activation by intracellular Ca^{2+}. Consistent with this was the finding that the sensitivity of $K_{Ca}2.2$(H337N) to activation by intracellular Ca^{2+} was not different from wild-type channels ($K_{Ca}2.2$(H337N), EC_{50} = 227 ± 8 nM; n_h = 5.61 ± 0.34). Our data indicate the primary role of the outer pore H residue in mediating the inhibition of macroscopic $K_{Ca}2$ current, which is at least in part mediated by a reduction in single-channel conductance. Consistent with the above data, the mutant channel $K_{Ca}2.2$(H337N) that was insensitive to $[H^+]_o$ inhibition, displayed only low conductance openings (10.7 ± 0.26 pS; n = 3) (Fig. 2 C), but with unchanged open-state kinetics (Fig. 3 C). This conductance state was very similar to both the lower

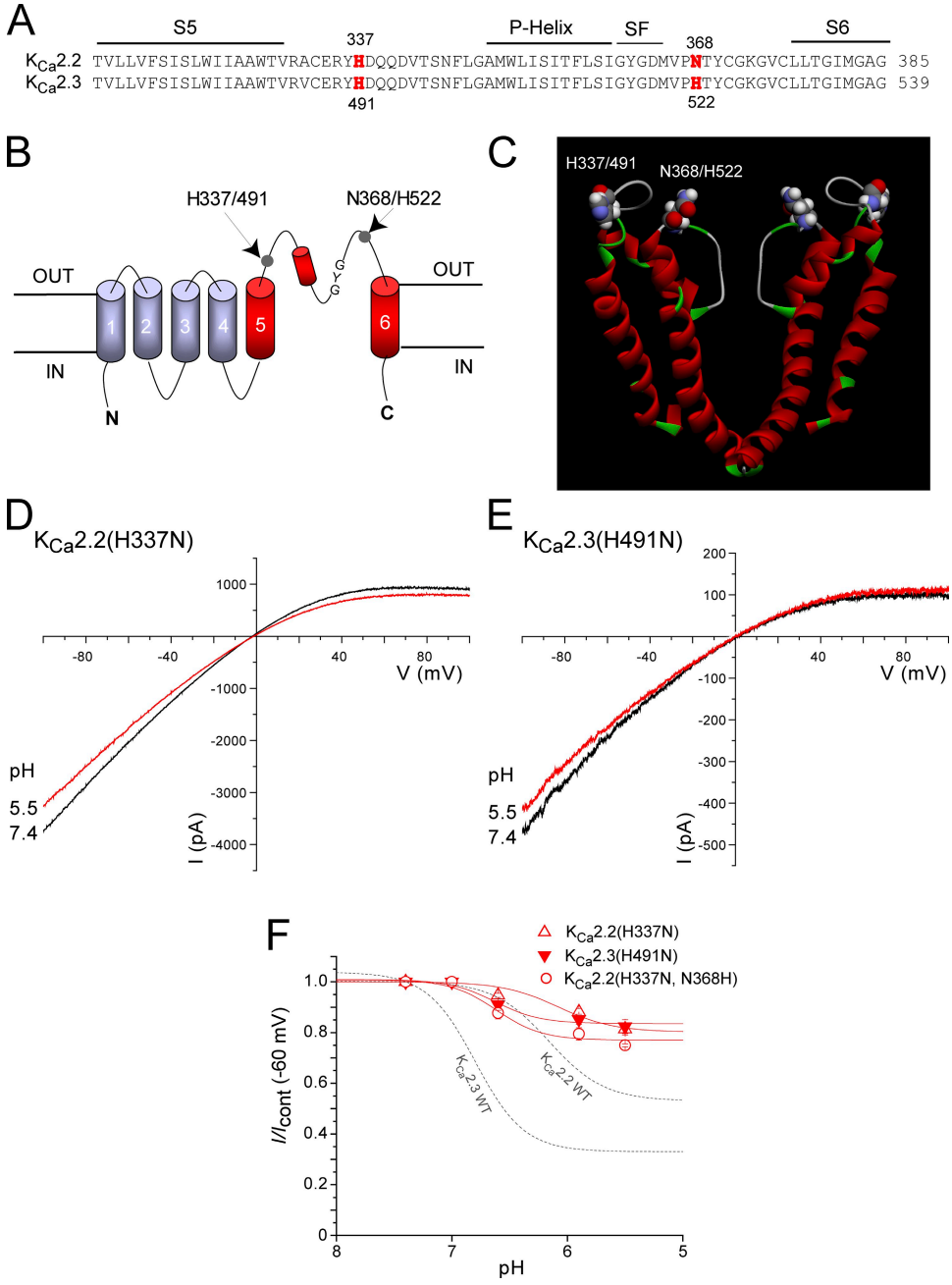

Figure 6. The outer pore histidine residue common to both $K_{Ca}2.2$ and $K_{Ca}2.3$ was crucial to block by $[H^+]_o$. (A) Sequence alignment of predicted outer pore region that spans the S5-P helix-SF-S6 of $K_{Ca}2.2$ and $K_{Ca}2.3$, with the single H residue in $K_{Ca}2.2$ and the two H residues in the pore of $K_{Ca}2.3$ highlighted. (B) Schematic representation of the location of the highlighted residues in $K_{Ca}2.2$ (H337 and N368) and $K_{Ca}2.3$ (H491 and H522). (C) Homology model of the pore region S5-P helix-SF-S6 of $K_{Ca}2.2$ displaying two subunits of the channel tetramer with proposed positions of the H and N residues labeled and represented in space-filled mode. Representative (D) $K_{Ca}2.2$(H337N) and (E) $K_{Ca}2.3$(H491N) outside-out patch currents evoked by a voltage ramp from −100 to +100 mV. Both channel mutants were poorly sensitive to inhibition by extracellular pH 5.5. (F) The concentration–inhibition relationships of currents measured at −60 mV of $K_{Ca}2.2$(H337N), $K_{Ca}2.3$(H491N), and $K_{Ca}2.2$(H337N, N368H). The sensitivity of wild-type currents is shown for comparison.

conductance states of wild-type $K_{Ca}2.2$ channels of 10.8 ± 1.4 pS (Fig. 2 A) (P = 0.94; n = 3), with a small but significant difference between the conductance of the mutant and the wild-type channel extracellular pH 5.9 (9.63 ± 0.07 pS; P < 0.02; n = 3). These data suggested that an uncharged basic H residue in the outer pore of $K_{Ca}2$ channels was required to maintain a high conductance state configuration of the pore. This proposal was supported by finding that mutation of H337 to the positively charged arginine residue (H337R) produced a channel whose conductance was estimated by nonstationary noise to be 11.9 ± 1.9 pS (n = 6; not depicted), a conductance significantly different from wild-type $K_{Ca}2.2$ channels (P < 0.05).

The presence of a second H residue in the pore region of $K_{Ca}2.3$ conferred extra sensitivity to $[H^+]_o$

It was postulated that the additional histidine residue (H522) located in the outer pore region of $K_{Ca}2.3$, but not $K_{Ca}2.2$, was responsible for the higher sensitivity of $K_{Ca}2.3$ current to extracellular protons. This was tested by mutating the outer pore regions of both $K_{Ca}2.2$ and $K_{Ca}2.3$ to mimic the sibling's pore. Therefore, N368 in $K_{Ca}2.2$ was mutated to a histidine (N368H) to mimic the $K_{Ca}2.3$ pore ($K_{Ca}2.2$(N368H)), and H522 in $K_{Ca}2.3$ was mutated to asparagine (H522N) to mimic the $K_{Ca}2.2$ pore ($K_{Ca}2.3$(H522N)). Both mutants produced functional current with properties consistent with $K_{Ca}2$ channel current (Fig. 7, A and B). The application of extracellular pH 6.6 to $K_{Ca}2.2$(N368H) showed a greater inhibition than wild-type $K_{Ca}2.2$ (Fig. 7 A). Conversely, $K_{Ca}2.3$(H522N) was less sensitive to extracellular protons than wild-type $K_{Ca}2.3$ current (Fig. 7 B). The generation of concentration–inhibition relationships for both mutants showed that $K_{Ca}2.2$(N368H) (n = 5) displayed a sensitivity to extracellular protons that mirrored (P = 0.91) wild-type $K_{Ca}2.3$ current (n = 11) (pIC_{50} of ∼6.9), shifting the pIC_{50} of $K_{Ca}2.2$(N368H) to 6.8 from 6.2 of wild-type $K_{Ca}2.2$ (Fig. 7 C). In contrast, the sensitivity of $K_{Ca}2.3$(H522N) to protons was significantly reduced (P < 0.0001; n = 3) (pIC_{50} of ∼6.4) when compared with wild-type $K_{Ca}2.3$ current (pIC_{50} of ∼6.9) (Fig. 7 C). These data strongly suggested that H522 in the outer pore region of $K_{Ca}2.3$ was responsible for the higher sensitivity to extracellular protons displayed by the channel.

The histidine–proton interaction sites do not form a high affinity Zn^{2+} binding site

Zinc ions (Zn^{2+}) bind to histidine and cysteine residues that are in specific conformations with a high affinity (Vallee and Auld, 1990). This binding has been shown to mimic the effects of extracellular protons interacting with H residues in voltage-gated K^+ channels

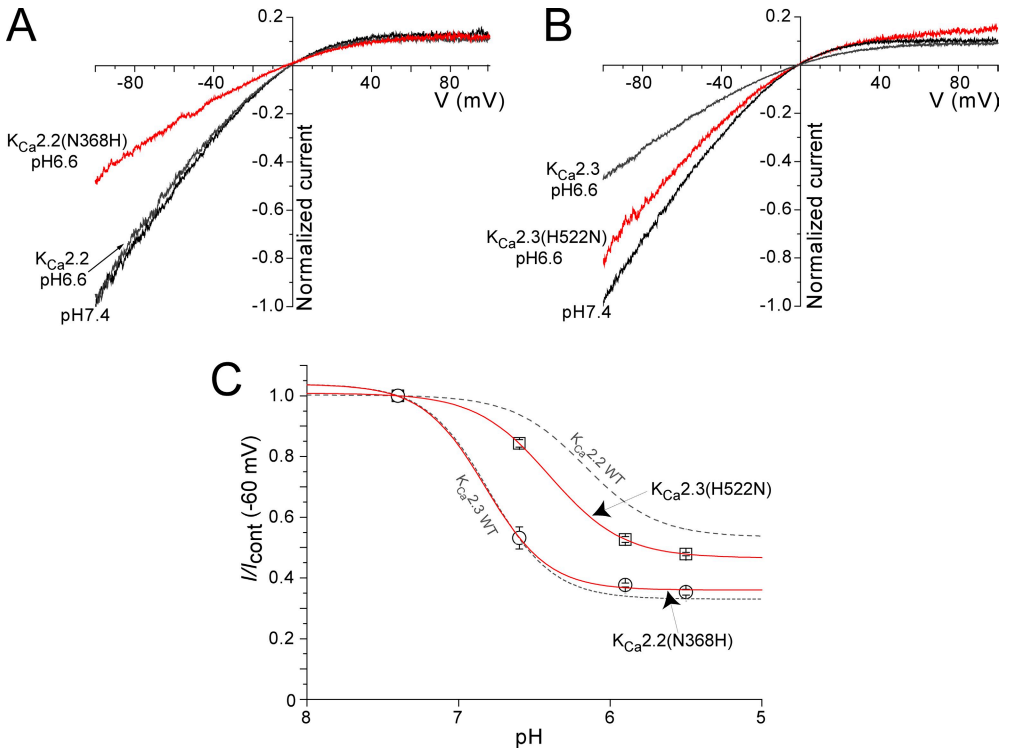

Figure 7. The second H residue within the outer pore region of $K_{Ca}2.3$ conferred extra sensitivity to $[H^+]_o$. (A) Ramp currents of wild-type $K_{Ca}2.2$ and the mutant $K_{Ca}2.2$(N368H) to mimic the outer pore sequence of $K_{Ca}2.3$ (in extracellular pH 7.4) were normalized to the maximum current at pH 7.4. The addition of extracellular pH 6.6 to wild-type $K_{Ca}2.2$ and the mutant $K_{Ca}2.2$(N368H) evoked no inhibition of wild-type current, but significant block of the mutant. (B) Mutation of the second H residue in $K_{Ca}2.3$ produced a channel current that was poorly sensitive to extracellular pH 6.6 when compared with the wild-type channel current. (C) The concentration–inhibition relationship for wild-type $K_{Ca}2.2$ and $K_{Ca}2.3$ currents, and mutants $K_{Ca}2.2$(N368H) and $K_{Ca}2.3$(H522N) currents by extracellular acidosis. Channel currents were measured at −60 mV and fitted with the Hill equation to yield the following: $K_{Ca}2.2$(N368H), IC_{50} = 160 ± 33 nM and pIC_{50} = 6.8; n = −2.13 ± 0.08 (reflecting the increased sensitivity to $[H^+]_o$ compared with $K_{Ca}2.2$, pIC_{50} = 6.16); and $K_{Ca}2.3$(H522N), IC_{50} = 688 ± 28 nM and pIC_{50} = 6.43; n = 2.08 ± 0.16 fit (showing the reduced sensitivity to $[H^+]_o$ when compared with $K_{Ca}2.3$, pIC_{50} = 6.8) (n = 3–5).

(Kehl et al., 2002). The effect of extracellular Zn^{2+} on the $K_{Ca}2.2$ channel current was tested to determine whether the outer pore H residue could act as a binding site of the divalent cation. The $K_{Ca}2.2$ current was not significantly inhibited at −60 mV by Zn^{2+} (4.5 mM), whereas $K_{Ca}2.3$ was significantly inhibited 38 ± 3.4% ($P < 0.01$) (Fig. 8, A and B). The difference in sensitivity between channel subtypes resulted from H522 in $K_{Ca}2.3$, as $K_{Ca}2.2$(N368H) showed an increased sensitivity (26.9 ± 2.9% block by 4.5 mM Zn^{2+}; $P < 0.01$) (Fig. 8 C) and $K_{Ca}2.3$(H522N) showed a significant reduction in block compared with the wild-type channel (0.4 ± 2.5% block by 4.5 mM Zn^{2+}; $P < 0.001$) (Fig. 8 D). These data suggest that Zn^{2+} could not coordinate at the H337/H498 residue, located in the outer pore between the S5-P helix, but could access and interfere with conduction by binding to the H in the pore at the SF-S6 segment (H522 in $K_{Ca}2.3$) with very low affinity.

Extracellular $[H^+]_o$ shifted inward rectification of $K_{Ca}2.3$ current to more depolarized potentials

The inhibition of macroscopic current by $[H^+]_o$ was voltage dependent, with less inhibition observed for outward current evoked positive to 0 mV (Fig. 1, A and B). However, resolving the inhibition of outward current was difficult to achieve because of the small amplitude and clear rectification that was observed under high K^+ conditions. The inhibition of both $K_{Ca}2.2$ and $K_{Ca}2.3$ current by extracellular protons was also observed in low K^+. $K_{Ca}2.2$ and $K_{Ca}2.3$ current recorded under low K^+ conditions showed clear inward rectification at membrane potentials positive to 0 mV. The application of extracellular protons inhibited both current types, but it also shifted the onset of inward rectification to more depolarized levels for the $K_{Ca}2.3$ current (Fig. 9, A and B). The concentration–inhibition relationships for the two channel subtypes showed that the sensitivity of current to protons was reduced in low K^+, with a shift of pIC_{50} of 6.2 in high K^+ to 5.6 in low K^+ for $K_{Ca}2.2$, and from pIC_{50} from 6.8 to 6.6 in $K_{Ca}2.3$ (Fig. 9 C). The small amplitude of the $K_{Ca}2.2$ current in outside-out patches made it unsuitable to obtain pIC_{50} values from individual experiments, with the fit being imposed onto meaned data. This prevented the determination of significance of the shift in sensitivity of the $K_{Ca}2.2$ current to protons between high and low K^+. However, the shift in sensitivity was significant for the $K_{Ca}2.3$ current ($P < 0.002$; $n = 6$–11).

It was clear that current inhibition was associated with a shift in inward rectification, especially for $K_{Ca}2.3$-mediated current (Fig. 9, A and B). The apparent voltage dependence of the rectification was characterized using a modified Goldman-Hodgkin-Katz (GHK) current equation. $K_{Ca}2$ channel currents do not display voltage dependence (Hirschberg et al., 1998), with inward rectification arising from block by intracellular Mg^{2+} ions (Soh and Park, 2001). Furthermore, $K_{Ca}2$ currents approach pure GHK rectification in the absence of intracellular Mg^{2+} (Soh and Park, 2001). Therefore, the current–voltage relationships of both $K_{Ca}2.2$ and $K_{Ca}2.3$ currents should follow the predicted deviation from the GHK equation due to rectification by internal divalent cations, including a term that describes the voltage dependence of block (Woodhull, 1973) by intracellular cations (Pusch, 1990) (Eq. 3):

$$I = P\frac{VF^2}{RT}\frac{[K^+]_i - [K^+]_o \exp\left(\frac{-FV}{RT}\right)}{1-\exp\left(\frac{-FV}{RT}\right)}\cdot\frac{1}{1+\frac{[Mg^{2+}]_i}{{}_{Mg^{2+}}K_d(0mV)\exp\left(\frac{-\delta zFV}{RT}\right)}}, \quad (3)$$

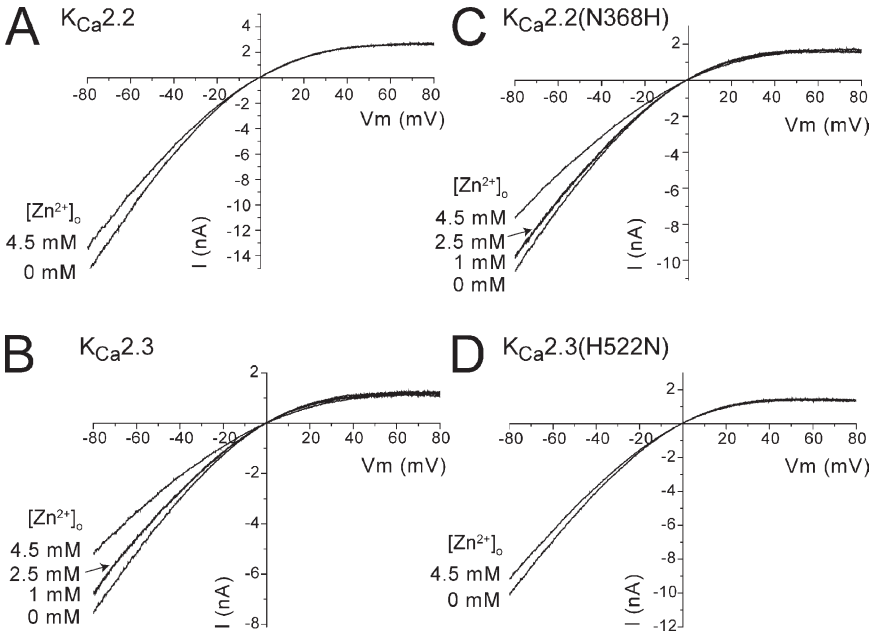

Figure 8. Extracellular Zn^{2+} accesses only the second H residue in $K_{Ca}2.3$ to cause moderate block. Representative whole cell currents of (A) $K_{Ca}2.2$ and (B) $K_{Ca}2.3$ channels evoked by voltage ramps from −80 to +80 mV under increasing concentrations of extracellular Zn^{2+}. $K_{Ca}2.3$ current was more sensitive to block by Zn^{2+} than $K_{Ca}2.2$. (C) Representative currents of the mutant $K_{Ca}2.2$(N368H) showing an increased sensitivity to Zn^{2+} compared with $K_{Ca}2.2$. (D) Showing the reduced sensitivity to Zn^{2+} of the mutant $K_{Ca}2.3$(H522N), a mutation to mimic the $K_{Ca}2.2$ pore sequence that lacked the second H found in $K_{Ca}2.3$.

where $^{Mg}K_d(0\ mV)$ is the apparent equilibrium dissociation constant for Mg^{2+} at 0 mV. The effect of $[Mg^{2+}]_i$ is represented as a first-order blocking mechanism dependent on voltage, whereas the fit parameter $^{Mg}K_d(0\ mV)$ is a measure of the degree of rectification with higher affinity values correlating with a stronger rectification. Fig. 9 D shows that the mean normalized currents for $K_{Ca}2.2$ measured every 20 mV at pH 7.4 and 5.5 were well described by Eq. 3 (the intermediate external pH data points are left out for clarity), revealing that extracellular protons had little effect on δ (0.19 at pH 7.4 compared with 0.16 at 5.5) or $^{Mg}K_d(0\ mV)$ (~0.01 mM). This suggests that the interaction of protons with $K_{Ca}2.2$ channels has little impact on the Mg^{2+} binding site and consequent rectification. Fitting the normalized $K_{Ca}2.3$ currents at pH 7.4 and 5.5 with Eq. 3 showed that extracellular protons had little effect on δ, but the $^{Mg}K_d(0\ mV)$ shifted from ~0.15 mM in pH 7.4 to 1.8 mM in pH 5.5 (Fig. 9 E). These results suggest that proton binding to $K_{Ca}2.3$ channels reduces the affinity of Mg^{2+} binding to the rectification site without shifting the position of the site within the membrane field.

It has been proposed that rectifying divalent cations bind to serine 359 in $K_{Ca}2.2$ channels, which is located at the intracellular mouth of the selectivity filter (Soh and Park, 2002). It is possible that protons might conduct through $K_{Ca}2.3$ channels and compete with intracellular Mg^{2+} ions for rectification. Values for $^{Mg}K_d(0\ mV)$ obtained from the fitting of Eq. 3 across the pH range (7.4–5.5) vary with pH and are fitted by the Hill equation with a pIC_{50} of 6.1 (Fig. 9 F). This pIC_{50} is similar to the pK_a of a histidine residue in solution as a single amino acid, which might suggest that the increase in $^{Mg}K_d(0\ mV)$ is mediated through a titration of a histidine exposed to the extracellular solution by protons, and not by direct competition with Mg^{2+} for the rectification site.

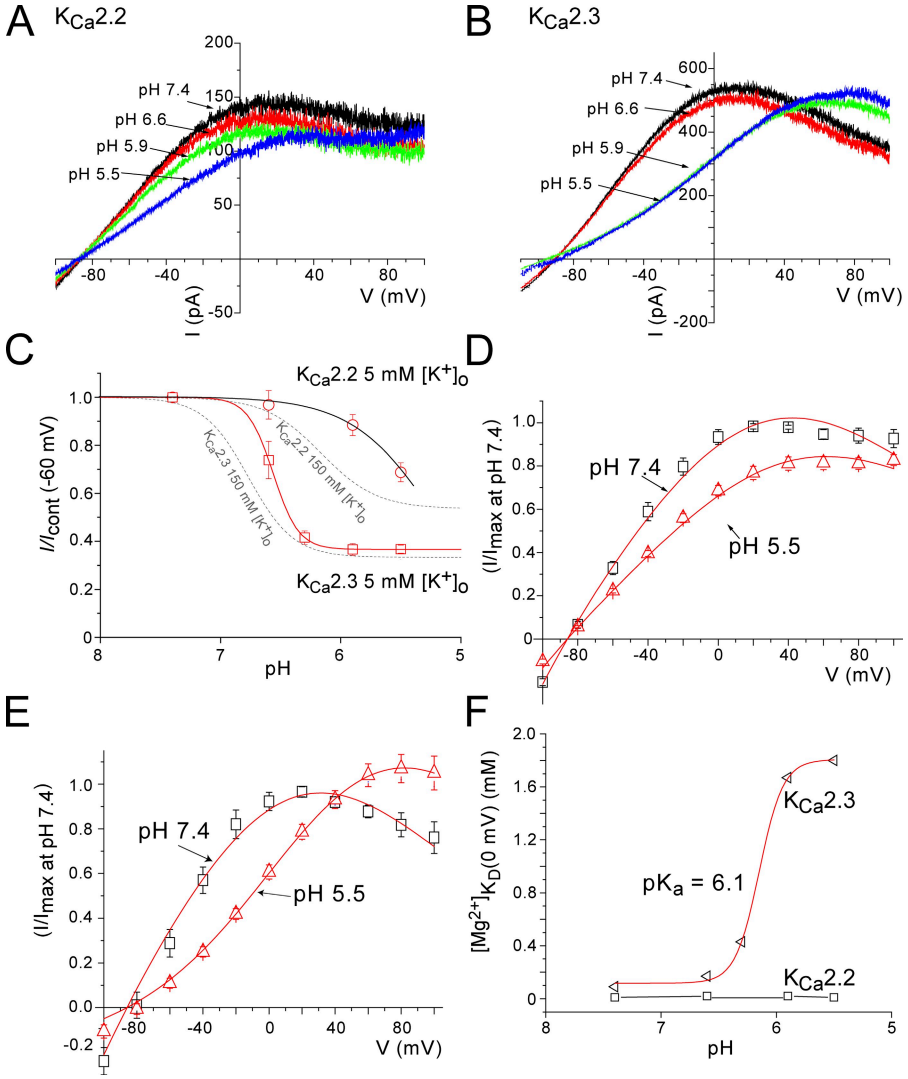

Figure 9. Extracellular $[H^+]_o$ shifts the inward rectification of $K_{Ca}2.3$ to more depolarized potentials. Representative outside-out macropatch (A) $K_{Ca}2.2$ and (B) $K_{Ca}2.3$ currents in low K^+ in the presence of increasing concentrations of $[H^+]_o$. Decreasing extracellular pH inhibited both current subtypes, with a shift of inward rectification apparent for the $K_{Ca}2.3$ current. (C) Concentration–inhibition relationships for $K_{Ca}2.2$ and $K_{Ca}2.3$ currents measured at −60 mV in both low K^+ (5 mM $[K^+]_o$) and high K^+ (150 mM $[K^+]$), showing that both $K_{Ca}2.2$ and $K_{Ca}2.3$ currents were less sensitive to $[H^+]_o$ in low K^+. Individual patches were fit with Eq. 1 to yield the following: $K_{Ca}2.3$, IC_{50} = 269 ± 16 nM and pIC_{50} = 6.6; n = −5.5 ± 0.16 (n = 3–6). $K_{Ca}2.2$ current was very small at −60 mV, only allowing meaned data to be fitted, yielding the following: pIC_{50} = 5.6; n_h = −1.88 (n = 4). The shift in the onset of rectification was illustrated fitting normalized currents with Eq. 3 for (D) $K_{Ca}2.2$: pH 7.4, δ = 0.19, and $^{Mg}K_d$ (0 mV) = 0.01 mM, and pH 5.5, δ = 0.16, and $^{Mg}K_d(0\ mV)$ = 0.01 mM, showing no effect on the affinity for the rectifying divalent ion by increasing $[H^+]_o$ and (E) $K_{Ca}2.3$: pH 7.4, δ = 0.22, and $^{Mg}K_d(0\ mV)$ = 0.09 mM, and pH 5.5, δ = 0.20, and $^{Mg}K_d(0\ mV)$ = 1.8 mM, showing a reduced affinity for intracellular divalent ions to evoke inward rectification at acidic extracellular pH. (F) The values of $^{Mg}K_d(0\ mV)$ from the fits of Eq. 3 over the full range of $[H^+]_o$ were plotted against pH and fitted with the Hill equation to give for pIC_{50} = 6.14 and n_h = 4.2 for $K_{Ca}2.3$, whereas $K_{Ca}2.2$ showed no shift in $^{Mg}K_d(0\ mV)$.

In addition, it suggests that the shift in rectification of the $K_{Ca}2.3$ current observed in low K^+ by lowering extracellular pH might result from protons interacting with the H522 that is unique to $K_{Ca}2.3$ (Fig. 6 A).

DISCUSSION

The presented data demonstrated that the protonation of an outer pore H residue common to both $K_{Ca}2$ channel subtypes mediated inhibition of macroscopic current. Extracellular acidification or mutation of the H residue did not affect channel activation by Ca^{2+}, indicating that protonation or mutation did not affect the structural requirements for gating. Inhibition of current was principally mediated by a decrease in single-channel conductance, associated with a depolarizing shift in current rectification in $K_{Ca}2.3$, and to a lesser extent in $K_{Ca}2.2$. This shift in rectification was produced by a reduction in the affinity of intracellular divalent ions for their proposed intracellular binding site (Soh and Park, 2002). These data indicated that the protonated outer pore H522 in $K_{Ca}2.3$ could be in the local electrostatic vicinity of the intracellular binding site (S359) for intracellular Mg^{2+} ions. Sensitivity to extracellular protons required the outer pore H residue common to both $K_{Ca}2$ channel subtypes, even though $K_{Ca}2.3$ possesses the additional H residue (H522). This was supported by the finding that the double-mutant $K_{Ca}2.2$(H337N, N368H) was also poorly sensitive to protons. This suggests that the first H residue acts to provide a specific molecular conformation that allows the second H to interact with protons to produce a shift in the rectification of $K_{Ca}2.3$. Finally, it was observed that $K_{Ca}2.3$(H522N) (a mutation to mimic the outer pore of $K_{Ca}2.2$) was more sensitive to extracellular protons than wild-type $K_{Ca}2.2$. This might suggest subtle differences in pore structure between the two wild-type channels.

It has been proposed that the pore structure of $K_{Ca}2$ channels shares close structural homology to Kv channels (Jäger and Grissmer, 2004). Superimposition of the pore sequence onto the crystal structure of Kv1.2 (Doyle et al., 1998; Long et al., 2005) suggested that H337 in $K_{Ca}2.2$ (within the S5-P helix loop) is a substantial distance away from the ion conduction pathway (Fig. 6 C). This would make it highly unlikely that the channel is subject to a direct occlusion/pore block by protonation of H337 (H491 in $K_{Ca}2.3$), and also unlikely to significantly electrostatically influence the conduction pathway. In addition, we observed that lowering external K^+ significantly reduced the sensitivity to proton inhibition, which is contrary to the competitive interaction with K^+ that would be expected if the H residue formed any part of the conduction pathway (Kehl et al., 2002; Fedida et al., 2005). This lack of competition also suggested that outer pore collapse (C-type inactivation), which is seen in Kv channels as the mechanism underlying inhibition, was not the mechanism for inhibition of $K_{Ca}2$ current, as this would also be antagonized by high K^+ (Baukrowitz and Yellen, 1995). It seems likely that inhibition of macroscopic current in $K_{Ca}2.2$ results from an indirect structural perturbation of the channel outer pore through H337 protonation. The protonation of H337 could change the local salt bridges and hydrogen bonds (Thompson et al., 2008) in a manner that couples to the structure of the conduction pathway. This allosteric effect could cause a change in pore shape resulting in lowered single-channel conductance, as the wild-type channel with H positively charged only displayed a conductance of ~11 pS, without affecting open-state kinetics. This hypothesis is supported by the reduced single-channel conductance that we observed for the $K_{Ca}2.2$(H337N) mutant channel. This is consistent with the proposal that a nonprotonated H residue in an outer pore position common to all $K_{Ca}2$ channels is necessary for maintaining a pore shape that permits high conductance openings, a pore shape not supported by a neutral or a positively charged amino acid. In $K_{Ca}2.3$, the extra sensitivity to protons is likely affected by the combination of structural perturbation through the protonation of S5-P helix H491 and the additional protonation of H522 causing further potential structural and electrostatic impairments to K^+ flux. Molecular modeling studies examining electrostatic interactions have supported experimental evidence that protonation of H residues in the outer pore perturb the electrostatic interactions of K^+ ions as they travel through the pore (Liu et al., 2007). The closer proximity of H522 than H491 to the $K_{Ca}2.3$ pore mouth might suggest that protonation of H522 could also contribute to inhibition through an electrostatic repulsion of K^+ in the outer pore region and conduction pathway.

The inhibition by protons displayed an apparent voltage dependence with less block at depolarized membrane potentials, an effect most pronounced for $K_{Ca}2.3$ current in low K^+. The fraction of inhibition at different voltages as a function of extracellular pH could not be fully described by the Woodhull model, which depicts a simple block of the permeation pathway by a charged ion (Woodhull, 1973). This might not be surprising, considering the arguments against protons acting as pore blockers discussed above. The lack of primary voltage dependence is also consistent with the prediction that both H residues would occupy positions in the outer pore region in areas not considered to be directly within the membrane field. We propose that protonated H522 interacted with the intracellular rectifying Mg^{2+} that is bound within the membrane field (Soh and Park, 2001). The affinity of the block by intracellular divalent ions to cause rectification varies with transmembrane voltage, $[Ca^{2+}]_i$, and $[K^+]_o$, suggesting the blocking ion is located in the conduction pathway (Soh and Park,

2001). To account for this, the currents were fit with a GHK equation modified to account for the voltage dependence of block by intracellular ions (Eq. 3) (Pusch, 1990). Our results suggested that the apparent voltage dependence of block by protons in $K_{Ca}2.3$ is a result of reducing affinity of intracellular divalent ions for the rectification binding site, with the estimated $^{Mg}K_d(0\ mV)$ from the fit shifting from 0.1 mM at pH 7.4 to 1.8 mM at pH 5.5. The electrical distance δ stayed about the same at ~0.2, suggesting that the location of the binding site in the field was not significantly shifted. The protonation-dependent change in pore shape, in addition to an electrostatic repulsive effect originating from the protonated H522, might perturb the configuration of the binding site for the divalent ion and lower affinity. Finally, the shift in rectification caused by extracellular protons was more pronounced in low K^+ than high K^+. It has been reported that increasing $[K^+]_o$ lowers the apparent affinity of the Mg^{2+} for the intracellular binding site through a mechanism commonly referred to as "*trans*-Knockoff" (Soh and Park, 2001). This proposal is consistent with the shift of rectification being more pronounced when the affinity for rectifying ions is higher (e.g., in low K^+). It is likely that the pore shape differs between $K_{Ca}2.2$ and $K_{Ca}2.3$ channels, which partly underlies the different sensitivity to extracellular protons. It is noteworthy that acidic pH is the only condition described so far that clearly inhibits $K_{Ca}2.3$ more than $K_{Ca}2.2$ channel currents. This knowledge may give hints for the development of future preferential $K_{Ca}2.3$ channel blockers.

Transient changes in extracellular pH occur during periods of physiological neuronal activity, such as synaptic activation (Chesler, 1990) and pathological events, such as epileptic seizures and cerebral ischemia (Chesler and Kaila, 1992; Tombaugh and Sapolsky, 1993), falling to below pH 6.5 during ischemia (von Hanwehr et al., 1986). Inhibition by acidosis would have effects dictated by channel subunit location. $K_{Ca}2.2$ and $K_{Ca}2.3$ channel subunits display distinct but overlapping expression patterns in the brain (Sailer et al., 2002, 2004). For example, $K_{Ca}2.2$ and $K_{Ca}2.3$ subunits are present in the hippocampus, with $K_{Ca}2.2$ present in dendrites and dendritic spines and $K_{Ca}2.3$ subunits localized in mossy fiber terminals (Sailer et al., 2002, 2004; Lin et al., 2008). Inhibition of spine-located $K_{Ca}2.2$ channel current during synaptic activation would aid the induction of long-term potentiation (Lin et al., 2008), whereas inhibition of channel current located in dendrites would increase excitability (Kelly and Church, 2004). In contrast, the inhibition of mossy fiber terminal $K_{Ca}2.3$ channel current would affect transmitter release and the induction of long-term potentiation at that synapse. It is clear that the differences in proton modulation of these channels could reflect a functionally relevant separation that might contribute to the physiological roles of the $K_{Ca}2$ channel subtypes in different brain regions.

We wish to thank Mr. Guillaume Drion, Prof. Andy Randall, and Dr. Jon Brown for helpful discussions on data analysis.

This work was funded by a grant from the Belgian Science Policy (IAP 6/31 to V. Seutin and N.V. Marrion). V. Seutin was also supported by grant 9.4560.03 from The National Fund for Scientific Research (Belgium). C. Lamy was supported by a FIRST-DEI grant (516131) from the Walloon region of Belgium.

Christopher Miller served as editor.

Submitted: 28 April 2009
Accepted: 11 September 2009

REFERENCES

Baukrowitz, T., and G. Yellen. 1995. Modulation of K^+ current by frequency and external $[K^+]$: a tale of two inactivation mechanisms. *Neuron.* 15:951–960. doi:10.1016/0896-6273(95)90185-X

Chesler, M. 1990. The regulation and modulation of pH in the nervous system. *Prog. Neurobiol.* 34:401–427. doi:10.1016/0301-0082(90)90034-E

Chesler, M., and K. Kaila. 1992. Modulation of pH by neuronal activity. *Trends Neurosci.* 15:396–402. doi:10.1016/0166-2236(92)90191-A

Claydon, T.W., M.R. Boyett, A. Sivaprasadarao, K. Ishii, J.M. Owen, H.A. O'Beirne, R. Leach, K. Komukai, and C.H. Orchard. 2000. Inhibition of the K^+ channel kv1.4 by acidosis: protonation of an extracellular histidine slows the recovery from N-type inactivation. *J. Physiol.* 526:253–264. doi:10.1111/j.1469-7793.2000.00253.x

Cohen, A., Y. Ben-Abu, S. Hen, and N. Zilberberg. 2008. A novel mechanism for human K2P2.1 channel gating. Facilitation of C-type gating by protonation of extracellular histidine residues. *J. Biol. Chem.* 283:19448–19455. doi:10.1074/jbc.M801273200

Combet, C., M. Jambon, G. Deléage, and C. Geourjon. 2002. Geno3D: automatic comparative molecular modelling of protein. *Bioinformatics.* 18:213–214. doi:10.1093/bioinformatics/18.1.213

Coulter, K.L., F. Périer, C.M. Radeke, and C.A. Vandenberg. 1995. Identification and molecular localization of a pH-sensing domain for the inward rectifier potassium channel HIR. *Neuron.* 15:1157–1168. doi:10.1016/0896-6273(95)90103-5

Dilly, S., A. Graulich, A. Farce, V. Seutin, J.F. Liegeois, and P. Chavatte. 2005. Identification of a pharmacophore of SKCa channel blockers. *J. Enzyme Inhib. Med. Chem.* 20:517–523. doi:10.1080/14756360500210989

Doyle, D.A., J. Morais Cabral, R.A. Pfuetzner, A. Kuo, J.M. Gulbis, S.L. Cohen, B.T. Chait, and R. MacKinnon. 1998. The structure of the potassium channel: molecular basis of K^+ conduction and selectivity. *Science.* 280:69–77. doi:10.1126/science.280.5360.69

Fedida, D., S. Zhang, D.C. Kwan, C. Eduljee, and S.J. Kehl. 2005. Synergistic inhibition of the maximum conductance of Kv1.5 channels by extracellular K^+ reduction and acidification. *Cell Biochem. Biophys.* 43:231–242. doi:10.1385/CBB:43:2:231

Geiger, D., D. Becker, B. Lacombe, and R. Hedrich. 2002. Outer pore residues control the $H(^+)$ and $K(^+)$ sensitivity of the Arabidopsis potassium channel AKT3. *Plant Cell.* 14:1859–1868. doi:10.1105/tpc.003244

Hartveit, E., and M.L. Veruki. 2007. Studying properties of neurotransmitter receptors by non-stationary noise analysis of spontaneous postsynaptic currents and agonist-evoked responses in outside-out patches. *Nat. Protoc.* 2:434–448. doi:10.1038/nprot.2007.47

Hirschberg, B., J. Maylie, J.P. Adelman, and N.V. Marrion. 1998. Gating of recombinant small-conductance Ca-activated K^+ channels by calcium. *J. Gen. Physiol.* 111:565–581. doi:10.1085/jgp.111.4.565

Jäger, H., and S. Grissmer. 2001. Regulation of a mammalian Shaker-related potassium channel, hKv1.5, by extracellular potassium and pH. *FEBS Lett.* 488:45–50. doi:10.1016/S0014-5793(00)02396-6

Jäger, H., and S. Grissmer. 2004. Characterization of the outer pore region of the apamin-sensitive Ca2+-activated K+ channel rSK2. *Toxicon*. 43:951–960. doi:10.1016/j.toxicon.2004.03.025

Kehl, S.J., C. Eduljee, D.C. Kwan, S. Zhang, and D. Fedida. 2002. Molecular determinants of the inhibition of human Kv1.5 potassium currents by external protons and $Zn^{(2+)}$. *J. Physiol.* 541:9–24. doi:10.1113/jphysiol.2001.014456

Kelly, T., and J. Church. 2004. pH modulation of currents that contribute to the medium and slow afterhyperpolarizations in rat CA1 pyramidal neurones. *J. Physiol.* 554:449–466. doi:10.1113/jphysiol.2003.051607

Köhler, M., B. Hirschberg, C.T. Bond, J.M. Kinzie, N.V. Marrion, J. Maylie, and J.P. Adelman. 1996. Small-conductance, calcium-activated potassium channels from mammalian brain. *Science.* 273:1709–1714. doi:10.1126/science.273.5282.1709

Kwan, D.C., D. Fedida, and S.J. Kehl. 2006. Single channel analysis reveals different modes of Kv1.5 gating behavior regulated by changes of external pH. *Biophys. J.* 90:1212–1222. doi:10.1529/biophysj.105.068577

Lin, M.T., R. Luján, M. Watanabe, J.P. Adelman, and J. Maylie. 2008. SK2 channel plasticity contributes to LTP at Schaffer collateral-CA1 synapses. *Nat. Neurosci.* 11:170–177. doi:10.1038/nn2041

Liu, B., D.R. Westhead, M.R. Boyett, and J. Warwicker. 2007. Modelling the pH-dependent properties of Kv1 potassium channels. *J. Mol. Biol.* 368:328–335. doi:10.1016/j.jmb.2007.02.041

Long, S.B., E.B. Campbell, and R. Mackinnon. 2005. Crystal structure of a mammalian voltage-dependent Shaker family K^+ channel. *Science.* 309:897–903. doi:10.1126/science.1116269

Prole, D.L., P.A. Lima, and N.V. Marrion. 2003. Mechanisms underlying modulation of neuronal KCNQ2/KCNQ3 potassium channels by extracellular protons. *J. Gen. Physiol.* 122:775–793. doi:10.1085/jgp.200308897

Pusch, M. 1990. Open-channel block of Na+ channels by intracellular Mg^{2+}. *Eur. Biophys. J.* 18:317–326.

Sailer, C.A., H. Hu, W.A. Kaufmann, M. Trieb, C. Schwarzer, J.F. Storm, and H.G. Knaus. 2002. Regional differences in distribution and functional expression of small-conductance Ca^{2+}-activated K^+ channels in rat brain. *J. Neurosci.* 22:9698–9707.

Sailer, C.A., W.A. Kaufmann, J. Marksteiner, and H.G. Knaus. 2004. Comparative immunohistochemical distribution of three small-conductance Ca^{2+}-activated potassium channel subunits, SK1, SK2, and SK3 in mouse brain. *Mol. Cell. Neurosci.* 26:458–469. doi:10.1016/j.mcn.2004.03.002

Shakkottai, V.G., I. Regaya, H. Wulff, Z. Fajloun, H. Tomita, M. Fathallah, M.D. Cahalan, J.J. Gargus, J.M. Sabatier, and K.G. Chandy. 2001. Design and characterization of a highly selective peptide inhibitor of the small conductance calcium-activated K+ channel, $Sk_{Ca}2$. *J. Biol. Chem.* 276:43145–43151. doi:10.1074/jbc.M106981200

Sigworth, F.J. 1980. The variance of sodium current fluctuations at the node of Ranvier. *J. Physiol.* 307:97–129.

Soh, H., and C.S. Park. 2001. Inwardly rectifying current-voltage relationship of small-conductance Ca^{2+}-activated K^+ channels rendered by intracellular divalent cation blockade. *Biophys. J.* 80:2207–2215. doi:10.1016/S0006-3495(01)76193-0

Soh, H., and C.S. Park. 2002. Localization of divalent cation-binding site in the pore of a small conductance $Ca^{(2+)}$-activated $K^{(+)}$ channel and its role in determining current-voltage relationship. *Biophys. J.* 83:2528–2538. doi:10.1016/S0006-3495(02)75264-8

Steidl, J.V., and A.J. Yool. 1999. Differential sensitivity of voltage-gated potassium channels Kv1.5 and Kv1.2 to acidic pH and molecular identification of pH sensor. *Mol. Pharmacol.* 55:812–820.

Stocker, M., and P. Pedarzani. 2000. Differential distribution of three $Ca^{(2+)}$-activated $K^{(+)}$ channel subunits, SK1, SK2, and SK3, in the adult rat central nervous system. *Mol. Cell. Neurosci.* 15:476–493. doi:10.1006/mcne.2000.0842

Stocker, M., K. Hirzel, D. D'hoedt, and P. Pedarzani. 2004. Matching molecules to function: neuronal Ca^{2+}-activated K^+ channels and afterhyperpolarizations. *Toxicon.* 43:933–949. doi:10.1016/j.toxicon.2003.12.009

Thompson, A.N., D.J. Posson, P.V. Parsa, and C.M. Nimigean. 2008. Molecular mechanism of pH sensing in KcsA potassium channels. *Proc. Natl. Acad. Sci. USA.* 105:6900–6905. doi:10.1073/pnas.0800873105

Tombaugh, G.C., and R.M. Sapolsky. 1993. Evolving concepts about the role of acidosis in ischemic neuropathology. *J. Neurochem.* 61:793–803. doi:10.1111/j.1471-4159.1993.tb03589.x

Ureche, O.N., R. Baltaev, L. Ureche, N. Strutz-Seebohm, F. Lang, and G. Seebohm. 2008. Novel insights into the structural basis of pH-sensitivity in inward rectifier K^+ channels Kir2.3. *Cell. Physiol. Biochem.* 21:347–356. doi:10.1159/000129629

Vallee, B.L., and D.S. Auld. 1990. Active-site zinc ligands and activated H2O of zinc enzymes. *Proc. Natl. Acad. Sci. USA.* 87:220–224. doi:10.1073/pnas.87.1.220

von Hanwehr, R., M.L. Smith, and B.K. Siesjö. 1986. Extra- and intracellular pH during near-complete forebrain ischemia in the rat. *J. Neurochem.* 46:331–339. doi:10.1111/j.1471-4159.1986.tb12973.x

Woodhull, A.M. 1973. Ionic blockage of sodium channels in nerve. *J. Gen. Physiol.* 61:687–708. doi:10.1085/jgp.61.6.687

Xia, X.M., B. Fakler, A. Rivard, G. Wayman, T. Johnson-Pais, J.E. Keen, T. Ishii, B. Hirschberg, C.T. Bond, S. Lutsenko, et al. 1998. Mechanism of calcium gating in small-conductance calcium-activated potassium channels. *Nature.* 395:503–507. doi:10.1038/26758